

AD-A250 881



AD _____

MEASUREMENT OF THE MAGNETIC AND ELECTRICAL ACTIVITY
OF INDIVIDUAL CELLS IN VITRO

MIDTERM REPORT

CHRISTOPHER C. DAVIS

DECEMBER 3, 1991



Supported by

U.S. ARMY MEDICAL RESEARCH AND DEVELOPMENT COMMAND
Fort Detrick, Frederick, Maryland 21702-5012

Contract No. DAMD17-90-Z-0052

University of Maryland
College Park, Maryland 20742

Approved for public release; distribution unlimited.

The findings in this report are not to be construed as an
official Department of the Army position unless so designated
by other authorized documents

92-14444

REPORT DOCUMENTATION PAGE			Form Approved OMB No. 0704-0188	
Public reporting burden for this collection of information is estimated to average 1 hour per response, including the time for reviewing instructions, searching existing data sources, gathering and maintaining the data needed, and completing and reviewing the collection of information. Send comments regarding this burden estimate or any other aspect of this collection of information, including suggestions for reducing this burden, to Washington Headquarters Services, Directorate for Information Operations and Reports, 1215 Jefferson Davis Highway, Suite 1204, Arlington, VA 22202-4302, and to the Office of Management and Budget, Paperwork Reduction Project (0704-0188), Washington, DC 20503.				
1. AGENCY USE ONLY (Leave blank)	2. REPORT DATE December 3, 1991	3. REPORT TYPE AND DATES COVERED Midterm 24 Sep 90 - 23 Sep 91		
4. TITLE AND SUBTITLE Measurement of the Magnetic and Electrical Activity of Individual Cells in vitro		5. FUNDING NUMBERS DAMD17-90-Z-0052 61102A 3M161102BS15 CE DA335569		
6. AUTHOR(S) Christopher C. Davis				
7. PERFORMING ORGANIZATION NAME(S) AND ADDRESS(ES) University of Maryland College Park, Maryland 20742		8. PERFORMING ORGANIZATION REPORT NUMBER		
9. SPONSORING/MONITORING AGENCY NAME(S) AND ADDRESS(ES) U.S. Army Medical Research & Development Command Fort Detrick Frederick, Maryland 21702-5012		10. SPONSORING/MONITORING AGENCY REPORT NUMBER		
11. SUPPLEMENTARY NOTES				
12a. DISTRIBUTION/AVAILABILITY STATEMENT Approved for public release; distribution unlimited		12b. DISTRIBUTION CODE		
13. ABSTRACT (Maximum 200 words)				
14. SUBJECT TERMS RA 3; Stimuli; Birefringence; Microwave monitoring; Cell magnetic fields; Cell electric fields; Squid			15. NUMBER OF PAGES	
			16. PRICE CODE	
17. SECURITY CLASSIFICATION OF REPORT Unclassified	18. SECURITY CLASSIFICATION OF THIS PAGE Unclassified	19. SECURITY CLASSIFICATION OF ABSTRACT Unclassified	20. LIMITATION OF ABSTRACT Unlimited	

SUMMARY

This progress report has two parts. The first part reports progress to date on the development of a common-path, optical heterodyne fiber sensor for remote monitoring of the electrically induced birefringence of cells and tissue. The second part is a report from Professor John P. Wikswo of Vanderbilt University, who is a sub-contractor on the University of Maryland contract. He is working on the development of a very small SQUID "NanoSQUID", which will allow monitoring of the magnetic fields from cells and tissues within about 2mm of tissue at physiological temperature. The SQUID is at $\sim 4K$.

EXTRINSIC OPTICAL HETERODYNE FIBER SENSOR

The principle of this sensor is that an electrooptically active medium placed at the end of the sensor will induce a differential phase shift between two offset laser frequencies propagating in the fiber. Since the fiber is only a means of delivering laser light to the sensor element, which will eventually be a cell, the sensor is referred to as "extrinsic."

We have substantially improved the stability and performance of our common-path, dual-frequency, optical heterodyne fiber sensor during the last several months. We have improved the launch optics, and obtained much greater stability of alignment of the system. This has been accomplished with the inclusion of some new Newport, high stability, stainless-steel fiber mounts, which have allowed us to retain alignment adjustability, but maintain alignment without drift for several hours.

Our principal interest during the last several months has been in improving the performance of the sensor for remote detection of birefringence. We have fabricated, with the aid of Harry Diamond Laboratories, a GaAs test integrated circuit with a gold-plated back surface and a front surface with a gold strip line pattern. When this circuit is activated it becomes birefringent, so that a polarized light beam passing near a surface stripline and reflecting off the back surface experiences a birefringent phase shift. This is essentially the method of non-invasive, high-speed GaAs circuit probing developed by Dave Bloom at Stanford. We focus light onto the GaAs with a GRIN lens that is integrated onto the remote end of the fiber (see below). By modulating the voltage applied to the stripline pattern on the



<input checked="checked" type="checkbox"/>
<input type="checkbox"/>
<input type="checkbox"/>
Codes
or
al

A-1

circuit we can synchronously detect the birefringent phase shift detected by the heterodyne sensor.

The performance of the sensor in this application has proved spectacular. We can obtain good signal-to-noise ratio detection with only about 10mV applied to the circuit, and can map with submicron spatial resolution the electric-field distribution in the GaAs substrate produced by the surface stripline pattern. We can raster scan the sensor across the surface of the GaAs and produce a 2-D map of its birefringent structure. Figure 1. gives an example of such a scan. We can see repeatable small features that clearly reflect factors such as: imperfect edges on the gold stripline, traces of gold that have not been removed by etching, and perhaps the effects of different doping densities that were produced in the GaAs during processing. This applications of our heterodyne fiber sensor may have some real practical utility in GaAs integrated circuit testing and characterization. These experiments on GaAs have proved very useful in characterizing and optimizing the performance of the sensor. We hope to soon perform the first tests of the sensor on electrically active tissue.

We have demonstrated the excellent common-path, common-mode rejection of our true heterodyne sensor by performing the measurements described above at the remote end of 2.5km of single mode fiber. We are not using polarization-preserving fiber yet the sensor retains excellent performance in the ambient laboratory environment. The only effect of the long fiber is to cause a slow fading of the signal, which can be restored with an adjustable half-wave plate at the launch end. We are in the process of automating this waveplate adjustment. If the fiber is abused, then this does produce a detected signal.

We are presenting our work on the remote probing of GaAs at OFS '92 in Monterey. A copy of the conference summary is appended to this report.

RECENT IMPROVEMENTS IN THE SENSOR

We have made the following recent improvements to the common-path optical heterodyne fiber sensor.

(1) Incorporation of a 1.3 micrometer Lightwave Electronics laser as the source. This wavelength was essential to allow us to probe GaAs. We also anticipate better reflection

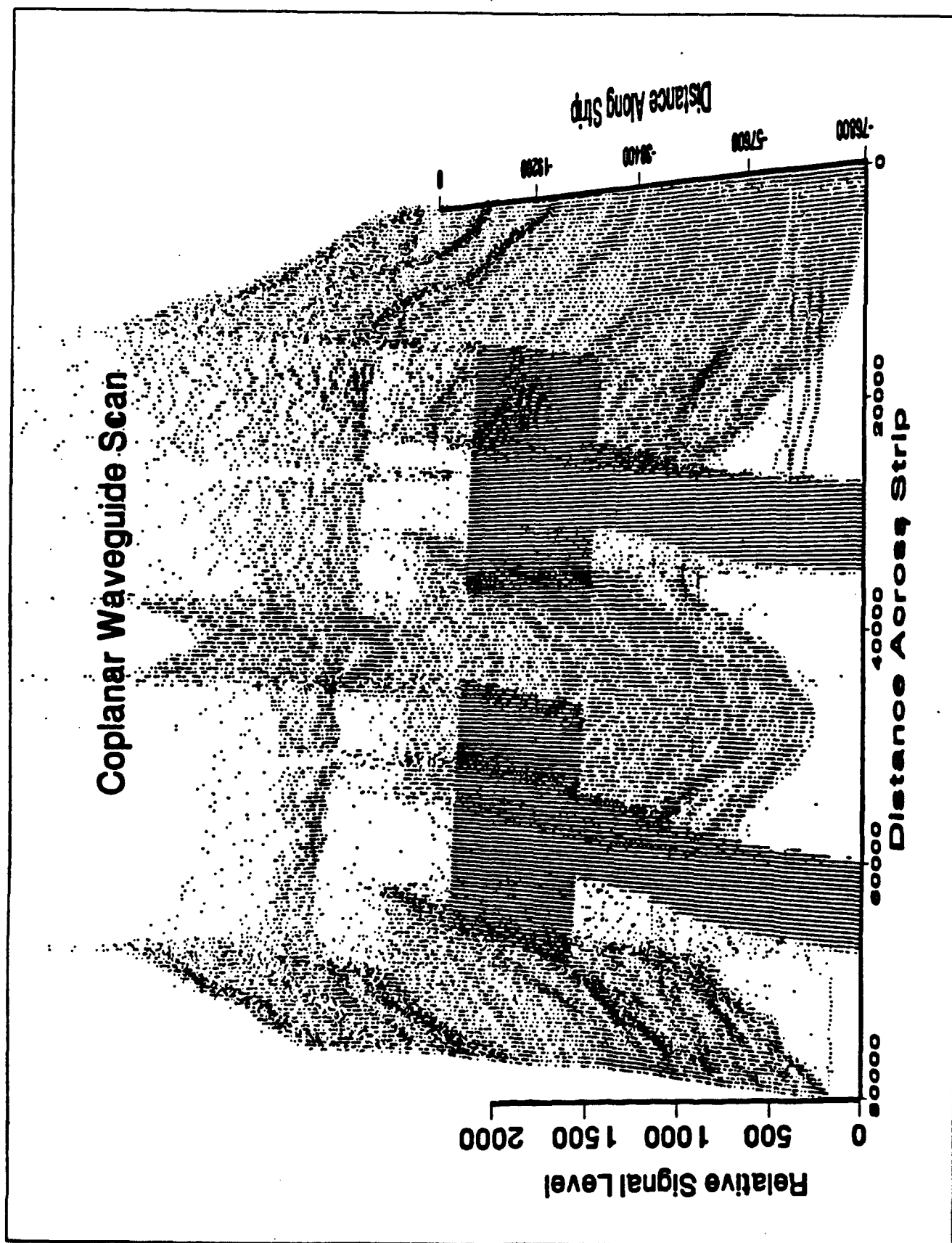


Fig. (1) 2-D Map of Electro-optic signal caused by birefringence in the surface of a GaAs integrated circuit.

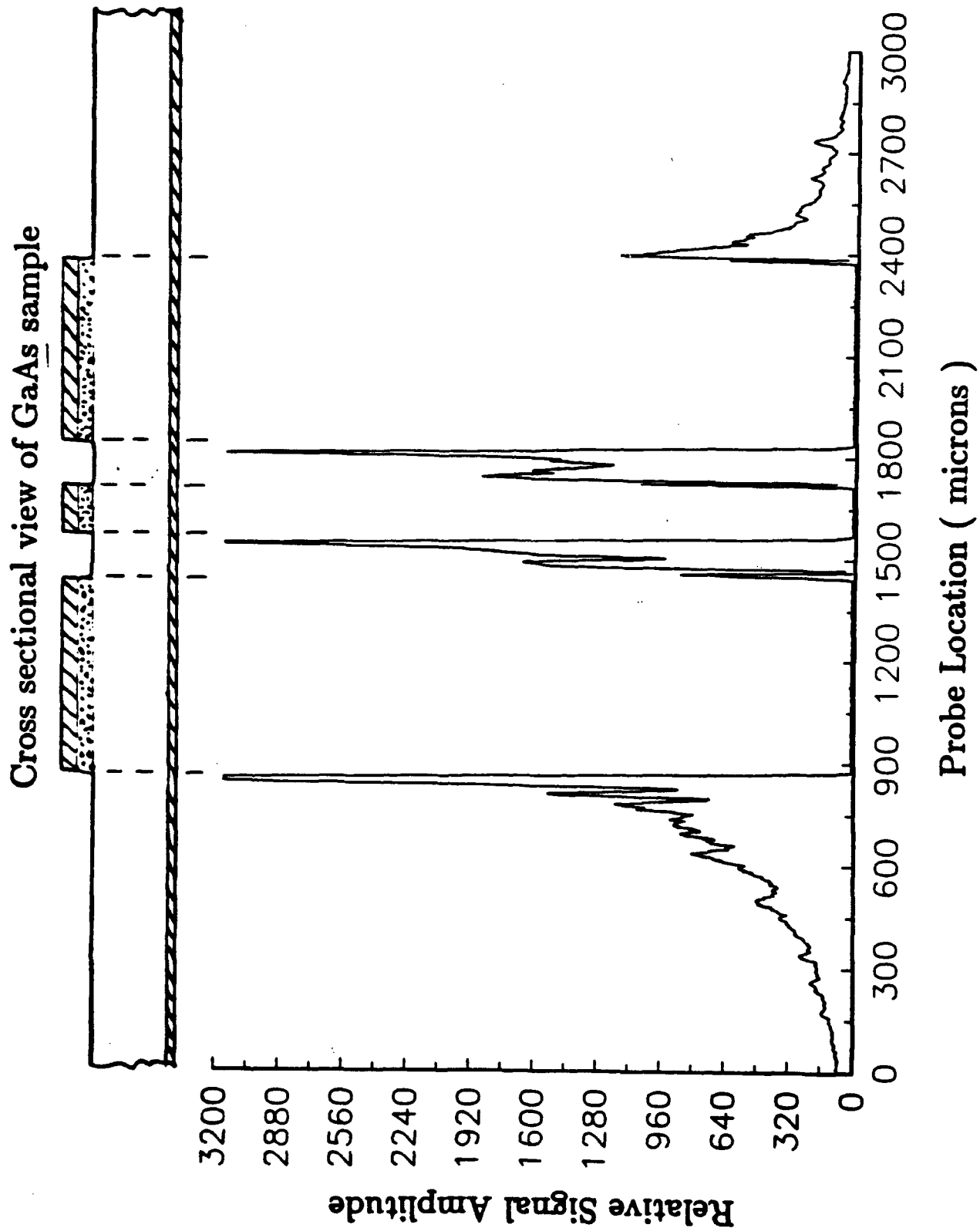


Fig.(2) 1-D scan of electric field distribution in surface of GaAs integrated circuit. The detailed features are real - they are not noise.

Extended Scan with
fiber polarization compensation



Fig.(3) Scan of electric field in surface of GaAs integrated circuit at the end of a very long fiber. Polarization compensation was used.

of this wavelength from the interfaces between the cell membrane and the cytoplasm, and the cell membrane and extra-cellular medium. Our present birefringence sensitivity is substantially greater than is expected to be necessary to detect cellular birefringence, the only unresolved question is how much light will make a double pass through the membrane and return into the fiber.

(2) We have developed a computer-controlled jig for alignment and epoxying of critical components and sub-assemblies of the system.

AUTOMATIC ALIGNMENT STAGE

This system is not quite in final form since we are still awaiting delivery of an A/D card for the computer that controls alignment. A PC clone is used and custom software has been written for the automatic alignment procedure. At present we have an improvised arrangement working that allows the adjustment of two sub-micron-step Klinger motorized stages for automatic alignment of fiber/component sub-assemblies. Certain problems developed during work on the automatic alignment stage that may be of interest.

(a) We started out using relatively conventional slow-curing epoxy for fixing components to fiber. The computer program was designed to continue small alignment adjustments during the curing time to compensate for creep. However, the epoxy hardens non-uniformly and the motor driven stages were found to be pushing the fiber into a tilted position with respect to the component to which it was being fixed. We have essentially eliminated this problem by disabling alignment adjustment after epoxy is applied, and by using UV-cured epoxy that hardens in a few minutes.

(b) The Klinger stages, which were sold to us as sub-micron precise adjusters, are only precise in this way during uni-directional adjustment. They have several microns of backlash. We feel that final piezoelectric adjustment would considerably reduce this backlash problem. It could also be reduced by incorporation of optical shaft encoders at considerable extra cost.

(c) Before fixing a cleaved end of a fiber to, for example, a GRIN lens, the fiber must be stripped. This produces, after epoxying, a weak point where the fiber tends to break. We

are now incorporating a plastic sleeve placed over the fiber whose end is also fixed to the optical component with epoxy.

PROGRESS REPORT
DEVELOPMENT OF NanoSQUID

DAMS1790Z0052

John P. Wikswo, Jr., P.I.
Department of Physics and Astronomy
Vanderbilt University
Nashville, TN

October 1991

The development of NanoSQUID involves three distinct tasks that are being pursued in parallel: the fabrication of the SQUID sensors and pickup coils, the integration of the SQUIDs with the commercial SQUID control electronics, and the optimization of the cryogenic system.

SQUID and Pickup Coil Fabrication.

The design and fabrication of the SQUID magnetometers and the gradiometer pickup coils for NanoSQUID are being conducted as a collaborative effort with IBM. We initially designed and fabricated a set of coils to be used with the old IBM d.c. SQUIDs developed by Claudia Tesche. However, we were forced to go to extreme measures to minimize a number of problems related to the impedance mismatch between the large inductance of the input coil on the SQUID chip and the very small inductance of the high resolution pickup coil. We had to construct an intermediate impedance-matching transformer and flexible superconducting leads to connect the pickup coils to the SQUID input coil. This, in turn, requires persistent-current joints between the pickup coils and the SQUIDs, and shielding of the intermediate lines and matching transformer from external fields. We fabricated prototypes of all of the required parts.

As a result of the problems intrinsic with this design, we decided instead to fabricate an entirely new integrated SQUID-pickup coil system, in which the input coil on top of the SQUID washer is matched directly to the low-inductance pickup coils. This provides a several-fold improvement in sensitivity due to the elimination of intermediate transformers, and leads to a significant reduction in the complexity of fabricating the entire system. We conducted extensive design simulations for the SQUID input and pickup coils, and we are presently preparing a manuscript describing our Monte Carlo optimization calculations.

Claudia Tesche has completed the layout of the new SQUID and pickup coil system, and the masks are presently being fabricated at IBM. A delay in our receiving the SQUIDs has arisen from the fact that a large number of other investigators at IBM have experimental devices to be incorporated into the same master mask set, and as a result, the entire design and fabrication process is rather slow. Future iterations should proceed more quickly. Claudia expects that we will receive the first SQUIDs within two months. Mark Ketchen, the physicist at IBM in charge of the fabrication of the SQUID chips, is a master SQUID builder and is producing thin-film dc SQUIDs using a new niobium tri-layer process. He is continuing to

refine the fabrication of the SQUIDs, and it is not yet clear whether their new process is fully optimized. One of the main justifications for waiting is that Ketchen's new SQUIDs are almost an order of magnitude quieter than those previously available at IBM, which are in turn a factor of two quieter than any commercially-available SQUIDs. Hence NanoSQUID, with these new SQUID sensors, should have a sensitivity that is comparable to our existing MicroSQUID, yet have a spatial resolution that is a factor of ten higher. Because of the reduced separation between the source and the pickup coils, we expect a factor of twenty-five stronger signal than we obtain with MicroSQUID. The resulting improvement in signal-to-noise ratio and spatial resolution that we will achieve should be phenomenal.

Because of the unanticipated delay with the delivery of the IBM SQUIDs, we began exploring a number of alternatives that would get NanoSQUID operational in the near term. Each alternative would utilize hand-wound pickup coils connected to a commercial SQUID sensor. This would allow us to make noise measurements on the existing NanoSQUID cryostat (see below). However, while we can wind pickup coils at Vanderbilt and could construct our own SQUID electronics, we cannot fabricate sufficiently quiet dc SQUIDs. As soon as this grant was funded, we decided to purchase commercial SQUID sensors and electronics, and began searching for the best vendor. In March, Quantum Design (QD) of San Diego announced a whole new line of high performance, low-cost SQUID sensors and electronics. In April, we ordered a single SQUID sensor and four channels of electronics from QD, with delivery scheduled for June. By May, they found that unexpected problems in their clean room were preventing them from reproducing their earlier high quality SQUIDs, and delivery was rescheduled for early winter.

We are now investigating alternative sources of SQUIDs. However, in the past six months, a number of actions by different commercial vendors have led to the virtual unavailability of SQUID sensors with matched electronics. Biomagnetic Technologies, Inc. (BTi) announced that it would no longer sell SQUIDs or electronics. Subsequently, it has been rumored that BTi is having trouble fabricating SQUIDs for use on its own magnetoencephalography systems! 2-G Associates of Mountain View CA produces electronics, but only sells Hypres, Inc. SQUIDs at high cost. We are entering into discussions directly with Hypres to obtain one of their d.c. SQUIDs for test purposes. If we are unable to obtain SQUIDs from either QD or Hypres, we will contact Conductus, Inc., a new superconducting electronics firm in California. Collaborators of ours on other projects are already working with Conductus to mount Conductus SQUIDs into QD SQUID housings. As a final alternative, and possibly the most fail-safe one, we can always construct the next prototype of NanoSQUID using an old R.F. SQUID sensor already in existence at Vanderbilt. In any case, we expect within the next six weeks to begin installation of one of the alternative SQUID systems into the NanoSQUID cryostat.

SQUID Electronics

Historically, 2-G Associates, QD, and BTi were the only vendors of d.c. SQUID electronics in the U.S. Each firm priced their electronics at \$10,000 per channel, making purchase of 4 systems for NanoSQUID problematic. IBM, the collaborator with the development of the NanoSQUID pickup coils, will not lend their electronics outside of their facilities. The well-engineered, and sophisticated d.c. SQUID preamplifier and control

electronics package offered by QD costs less than \$5,000 per channel. As soon as we identify our alternative source of dc SQUIDs, we will accept delivery on one set of QD electronics. When we have demonstrated a functioning SQUID sensor and SQUID electronics system at Vanderbilt, we will then proceed to mount this system in the NanoSQUID cryostat for magnetometer tests.

Cryogenic System

We are beginning the final preparations for the cryogenic tests of the NanoSQUID cryostat. We have finally obtained glass-encapsulated platinum thermometers that are nonmagnetic and will be suitable for temperature sensing in the NanoSQUID cryostat. We have already demonstrated the use of these thermometers in a closed-loop temperature control system based upon a Lakeshore temperature controller. An aluminum heat exchanger is being fabricated in the shop to be used on the initial tests with hand-wound pickup coils, reserving the more fragile and expensive quartz cold fingers for the tests with the thin film-IBM SQUIDs.

As soon as the initial tests are complete, we will proceed to modify the NanoSQUID cryostat and the QD SQUID housing that contains the input/output impedance matching transformers connecting the SQUID to the preamplifier circuits. Because the thin-film IBM SQUIDs are mounted directly on the chip with the pickup coils, the connections between the SQUIDs and the room temperature preamplifier simply involve connecting the appropriate current and voltage leads from the SQUID chip to the input/output transformers. In the conventional QD system, the SQUID and impedance matching circuitry are enclosed in a superconducting shield. A clever connector arrangement makes it possible to detach the SQUIDs from the cryogenic cable and preamplifier electronics. We will modify this housing to allow us to install the shielded matching transformers in the immediate vicinity of the cryogenic sections of NanoSQUID.

Once NanoSQUID is operational, we will proceed to characterize its spatial resolution and field sensitivity. We will then modify the system to optimize its performance. Finally, we will utilize NanoSQUID to make ultra-high resolution maps of action currents in a variety of biological systems.

TO BE PRESENTED AT THE CONFERENCE ON OPTICAL FIBER SENSORS
OFS '92, Monterey, California, Jan 29-31, 1992

**A Hybrid Coherent Fiber-Optic Probe for Remote
Sensing of Electro-Optic Effects in GaAs**

by

David L. Mazzoni, Kyuman Cho, Stephen Sadow, and Christopher C. Davis

**Electrical Engineering Department
University of Maryland
College Park, MD 20742
ph. (301) 405-3637**

Abstract

We present a very sensitive fiber interferometric sensor for remotely monitoring electro-optic effects in GaAs. This technique can be used for the analysis and characterization of GaAs components without the need for elaborate testing equipment and procedures.

A Hybrid Coherent Fiber-Optic Probe for Remote Sensing of Electro-Optic Effects in GaAs

by

David L. Mazzone, Kyuman Cho, Stephen Sadow, and Christopher C. Davis

Electrical Engineering Department
University of Maryland
College Park, MD 20742

Summary

It is well known that GaAs has a large electro-optic (EO) coefficient. Therefore, GaAs integrated circuits and devices can be probed optically through the electro-optic effects produced by steady or transient voltages in the circuit. For example, Bloom et al ⁽¹⁾ have shown that noninvasive electro-optic sampling of microwave circuits is useful for measuring device parameters. GaAs circuits can be tested using a transmission line formed on an electro-optic substrate. EO crystals are placed close to the device under test, and a sampling beam probes the crystal to measure the fringing fields of the transmission line. Unfortunately, this technique has limitations since the transmission line and crystal disturb the fields in the device under test. Techniques for non-perturbing in situ measurements, such as those investigated by Bloom, are more desirable since an external crystal is not required.

We have developed a coherent fiber-optic probe that is ideal for measuring birefringence in a remote sample. By utilizing a single fiber carrying two orthogonally polarized beams to a remote sensing section, the fading problem common to interferometers with separate beam paths is minimized. We employ phase locked loop detection which is insensitive to slowly varying phase shifts while at the same time being simple and inexpensive. Such sensors are ideal for the remote sensing of parameters in hostile environments or where electromagnetic fields can interfere with traditional sensors⁽²⁾.

In our implementation of a coherent hybrid sensor, in order to minimize phase and polarization drifts that occur when independent signal and reference arms are used in an interferometer, we have combined two orthogonally polarized beams into a single fiber, thereby minimizing common-mode effects. In addition, to avoid operating point drift that plagues homodyne detection schemes, we have used a true heterodyne scheme in which these two orthogonally polarized beams are at different frequencies. A single mono-mode fiber acts to deliver and return the beams to/from a remote sensor element. In GaAs circuit characterization the semiconductor substrate becomes the sensor element. It induces

a phase shift between the orthogonally polarized components of the beam penetrating the substrate. The beam is reflected off the back surface of the substrate into the fiber. The detection optics and electronics can be located in a benign location at the input end of the fiber. This type of single fiber system is relatively invulnerable to environmental effects since any perturbation effects both beams in the fiber, and any common mode signals can be suppressed in the detection electronics.

A diagram of the fiber sensor is shown in Figure 1. A 35 mW single mode diode pumped 1.3 μ m Nd-Yag laser is used as a signal source. The beam is optically isolated and passes through a 40 MHz Acousto-Optic modulator (AOM) that produces two beams, one of which is shifted in frequency by 40 MHz from the fundamental. The beams enter an arrangement of mirrors and $\lambda/2$ waveplates that align the beams with the first polarization sensitive beam splitter (PSBS1). One of the beams is also rotated 90° with respect to the other so that two collinear orthogonally polarized beams emerge from PSBS1. These beams are injected into a single mode fiber through a 3dB coupler. One of the coupler output beams is lost into index matching fluid, while the other output beam continues to the sensing end. A 0.29 pitch graded index (GRIN) lens is epoxied to the end of the fiber with a focal point 5 mm from the GRIN lens. The GRIN is positioned above the GaAs sample for maximum reflection. A computer controls an XYZ positioner that scans the GRIN above the GaAs device. The local electric field in the GaAs modulates the birefringence of the substrate and induces a phase shift between the orthogonal components of the probe beam. The beam is reflected back into the fiber and returns through the 3dB coupler, a $\lambda/2$ waveplate, and polarizing beam-splitter PSBS2 before reaching the detection photodiodes. The phase shift induced by the GaAs is detected by placing the output beam splitter (PSBS2) at 45°, so that the two orthogonal components of the beam mix. Final detection occurs at a balanced mixer using two wideband photodiodes. Common mode amplitude noise is suppressed by differentially amplifying the signals from these two photodiodes.

The output of the differential amplifier following the diodes in Fig.1 is

$$I_{diff} \propto \cos(\Delta\omega t + \Delta\phi_s - \phi_m) \quad (1),$$

where $\Delta\omega = \omega - \omega'$ is the AOM excitation frequency, ϕ_m is the induced phase shift, and $\Delta\phi_s$ is the static phase term. The signal modulation is present in ϕ_m and is directly detected in the PLL stage. The $\Delta\phi_s$ above represents a static phase shift due to differing path lengths, thermal expansion and contraction of the optical components, and other slowly varying effects. Heterodyne detection is immune to these pseudo-static phase perturbations. Direct PLL detection does not require a stable source since a voltage controlled oscillator is locked to the carrier. Although other schemes exist for heterodyne detection⁽³⁾, they often require complicated techniques and are usually not as sensitive as true heterodyne methods.⁽⁴⁾

The simplicity of the detection electronics using the direct PLL method is evident from Figure 1. The 40 MHz phase modulated signal from the photodiodes is amplified in a wide-band differential amplifier (ComLinear CL231). Using two diodes in a balanced detector arrangement improves the SNR by 3 dB - in addition, balanced detection suppresses amplitude noise from the laser. In Figure 1 the phase modulation is detected in a discrete 40 MHz PLL employing a limiter/AGC, doubly balanced mixer, 40 MHz VCO, and an active loop filter. Phase demodulation is achieved by mixing the differential amplifier output with the VCO output. The mixer output is filtered and is used to form the VCO control voltage that keeps the VCO frequency locked to the incoming RF carrier. The VCO control voltage also contains the demodulated phase signal, which is further amplified before the output signal is displayed on an oscilloscope or dynamic signal analyzer. This detection scheme is elegant and does not require any specialized or expensive components, making the sensor desirable for commercial applications.

Figure 2 shows the result obtained in scanning the fiber probe in one dimension perpendicular to 3 different gold stripline features on the surface of a GaAs (100) wafer. All three striplines were excited with a 4 kHz signal at 5V. The wafer underside was gold coated for enhanced reflection and used as a ground plane. At each of the outer electrodes the rising signal is due to the increase in electric field intensity adjacent to the gold striplines. In principle, this plot shows the electric field profile in the GaAs surrounding the electrodes. The results of Figure 1 show rough edges on the gold strips caused by wet chemical etching of the wafer, and this data is exactly reproducible. Furthermore, this technique can show extremely small variations in such things as conductor width, doping density, epitaxial layer differences, surface impurities, and defects in the GaAs.

Figure 3 shows a spectrum analyzer plot of the sensor signal obtained with a 5V signal on the stripline. A signal to noise ratio of at least 45dBV² is shown indicating that minimum sensitivities down to $\sim 7\text{mV}/\sqrt{\text{Hz}}$ can be achieved.

This research is supported by the U. S. Army Medical Research and Development Command through Contract DAMD-90-Z-0052. Stephen Sadow is also at Harry Diamond Laboratories, Adelphi MD.

References

;;

- [1] B. H. Kolner, D. M. Bloom, IEEE J. Quantum Electronics, QE-22, no.1 (January 1986).
- [2] D. L. Mazzoni, K. Cho, C. C. Davis, Optics Letters, 16 no.8 (April 1991)
- [3] T. Okoshi, IEEE J. Lightwave Technol., LT-3 no.6, (December 1985).
- [4] I. M. I. Habbab, and L. J. Cimini, Jr., IEEE J. Lightwave Technol., 6-10, (October 1988).

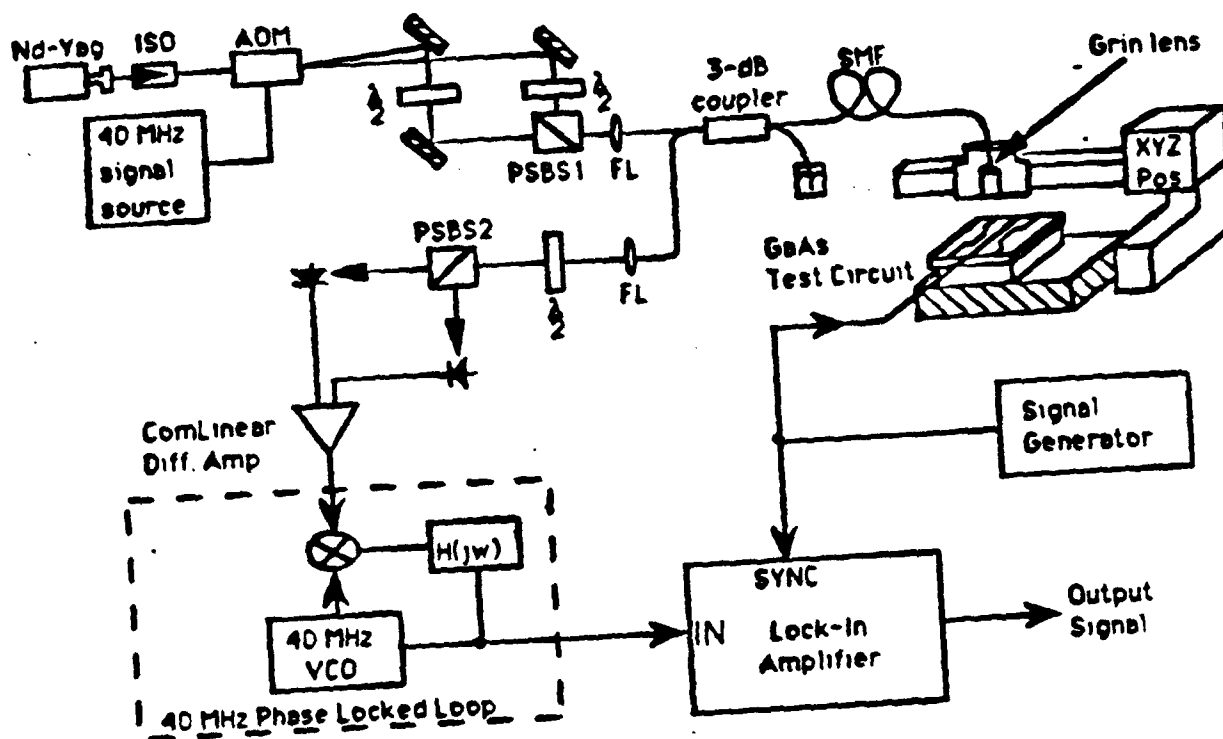


Figure 1. Coherent Hybrid Fiber-Optic Sensor

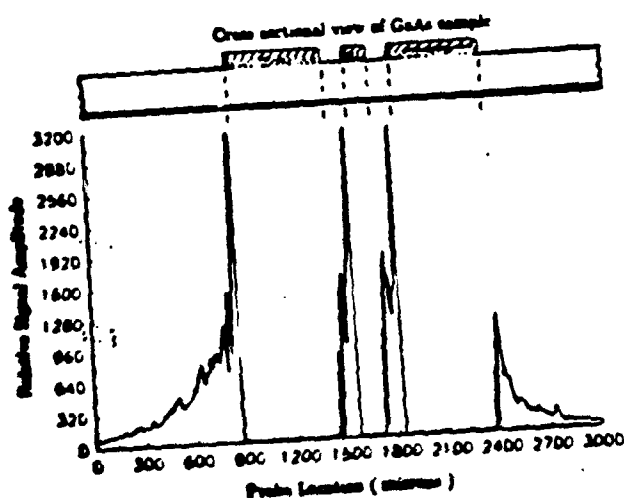


Figure 2
GaAs Scan Results

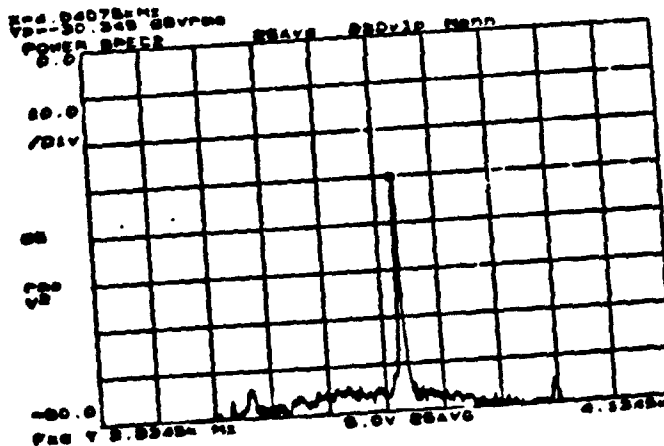


Figure 3
Signal Power Spectrum